Water Research 148 (2019) 106–114

Contents lists available at ScienceDirect

Water Research

journal homepage: www.elsevier.com/locate/watres

Synergistic effects of various in situ hydrolyzed aluminum species for the removal of humic acid

Jina Song [a, b], Pengkang Jin [b, *], Xin Jin [b], Xiaochang C. Wang [b]

[a] College of Energy and Environmental Engineering, Hebei University of Engineering, Handan, Hebei Province, 056038, China
[b] School of Environmental and Municipal Engineering, Xi'an University of Architecture and Technology, Xi'an, Shaanxi Province, 710055, China

ARTICLE INFO

Article history:
Received 1 August 2018
Received in revised form
9 October 2018
Accepted 13 October 2018
Available online 17 October 2018

Keywords:
Humic acids
Aluminum hydrolysis
Synergistic effects
Complexation capacity

ABSTRACT

Due to the diversity of in situ hydrolyzed aluminum species and discrepancy in the binding sites of humic acid (HA), the mechanisms involved in HA removal were significantly different in inorganic particle removal. Based on the background, the coagulation behavior of in situ and performed hydrolyzed aluminum species for the removal of HA was investigated. For $AlCl_3$, the maximum HA removal reached at weak acidic conditions, where various in situ hydrolyzed Al species containing Al_1 to Al_{20} cores with different amounts of water molecules were present. Various Al species could meet the demand for different binding sites and enhance the complexing probability for weak binding sites. Meanwhile, most of the binding sites are occupied by the aluminum ion, which brought about better complexation capacity with the Al species. Therefore, the synergistic effects of various in situ hydrolyzed aluminum species played important roles in the removal of HA. Compared with $AlCl_3$, preformed Al_{13} had less efficient in HA removal because the Zeta potential of HA formed by preformed Al_{13} with uniform Al species increased from negative to positive with increase in Al_{13} dosage. This study provided new insight into the interaction between HA and various hydrolyzed Al species.

1. Introduction

Coagulation is a widely applied unit process for removing particles and organic matter during the treatment of drinking water (Xu et al., 2010). Earlier research suggested coagulation mechanisms including double-layer compression and adsorption-neutralization for explaining inorganic particles destabilization (Black and Chen, 1965; Singley et al., 1971). Packham (1963) proposed that sweep coagulation occurred with formation of amorphous aluminum hydroxides in 1963. Prior to the 1960s, many investigations dealt with removing color from water to improve its aesthetic value. The research object of coagulation gradually focused on removing humic acid (HA) from water when it was discovered that the reaction of HA with free chlorine produced THMs and other by-products in 1970s (Randtke, 1988). People have realized that the mechanisms involved in HA removal were significantly different inorganic particle removal. Therefore, many researchers made great efforts to explain the difference between coagulation of HA and inorganic particle, and found that complexation reaction was an important in the coagulation process based on traditional theory (Angelico et al., 2014; Benschoten and Edzwald, 1990; Cheng and Chi, 2002; Lin et al., 2014; Lu et al., 1999). However, most studies still used the traditional coagulation mechanisms to explain the reaction between HA and aluminium salts.

As is well known, HA is a complex matrix of a heterogeneous mixture of organic substances with a high content of functional groups including carboxyl (-COOH), hydroxyl (-OH), and carbonyl (-C=O) groups (Bahemmat et al., 2016). The distribution of binding sites in HA could change due to differences in the type, number, and positions of functional group substituents on the benzene ring. Obviously, traditional theory was inapplicable to HA removal, as charges of inorganic particles are uniform under certain conditions which result in simplex interaction with hydrolyzed aluminum species. According to physical chemistry, these binding sites could act as Lewis base in solution. The stronger Lewis base of binding site is, the greater reactivity to form the complex through coordinate bond. So the binding site in HA with higher affinity could preferentially react with Al salts. Almost no research has been performed to investigate the reaction behaviour between HA and Al salts from the viewpoint of the discrepancy in the binding sites of humic acid.

---

* Corresponding author.
E-mail address: pkjin@hotmail.com (P. Jin).

https://doi.org/10.1016/j.watres.2018.10.039

On the other hand, aluminum salts coagulant can be hydrolyzed to different dissolved species in aqueous solution, which play significant roles in removing HA. During hydrolysis of $AlCl_3$, the hydrolyzed species included Al_a (mainly monomeric species, dimers, trimers, and some small polymers), Al_b (mainly $Al_{13}O_4(OH)_{24}^{7+}$, often denoted Al_{13}), and Al_c (mainly $Al(OH)_3$) (Yan et al., 2007). This spontaneous hydrolysis process is referred to as in situ hydrolysis. Various hydrolyzed aluminum species are formed by in situ hydrolysis of aluminum chloride, resulting in diverse affinities and complexation capacity between HA and Al species. It can therefore be assumed that various Al species could meet the demand for different binding sites and enhance the complexing probability for weak binding sites, which improves coagulation efficiency. However, few studies have considered the diversity of in situ hydrolyzed aluminum species, and investigated the difference affinity and complexation capacity between HA and aluminum due to the protonation/deprotonation characteristics of functional groups and in situ hydrolysis of Aluminum.

Although many studies claimed polyaluminum chloride (PACl) to be superior to traditional aluminum coagulants in terms of turbidity and natural organic matter (NOM) removal (Yan et al., 2008a; Tang and Luan, 1995), few studies have considered the limitations of simplex preformed Al species and the difference of coagulation behavior between preformed Al species and $AlCl_3$. Al_{13} was regarded as the most active species in PACl responsible for coagulation (Xu et al., 2011). Although the charge of preformed Al_{13} was high, the affinities to bind with all binding sites were almost equal. In view of this point, it can be deduced that preformed Al_{13} first bound with strong binding sites which result in partial supersaturation of sites and charge reversal and less efficient in HA removal. Therefore, the distinct performances of preformed Al_{13} and in situ generated Al species during coagulation needs further investigation.

To gain better understanding of the coagulation behaviour of in situ hydrolyzed and preformed Al species, ^{27}Al NMR and electrospray ionisation/mass spectroscopy (ESI-MS) were applied to investigate the distribution and performance of Al species of preformed Al_{13} and $AlCl_3$ at different pH during the coagulation process. Differential absorbance spectroscopy (DAS) was employed to quantitatively study HA-Al interactions with changes in Al dosage and pH. To investigate the reactivity of HA with coagulants, Py-GC-MS was used to monitor the different compounds of HA removed by preformed Al_{13} and $AlCl_3$. Based on experimental data, this study provides insight into coagulation mechanisms for HA removal by Al_{13} and $AlCl_3$ at different pH values.

2. Materials and methods

2.1. Materials and reagents

Humic acid was obtained from Sigma-Aldrich. Stock HA solution was prepared by adding 1 g HA into 1 L 0.1 mol/L NaOH solution. After stirring for 12 h, the samples were filtered through a 0.45 μm membrane to remove suspended materials.

For the preparation of Al_{13}, PACl was adopted as the primary material. A 100 mL 1.36 mol/L $AlCl_3 \cdot 6H_2O$ solution was titrated slowly with 240 mL of 1.36 mol/L NaOH solution within 5 h under rapid stirring conditions. After preparation, the solutions were set for at least 24 h of aging at room temperature. Polyaluminum chloride solution with a concentration of 0.4 mol/L and basicity of 2.4 was obtained.

The purification of Al_{13} was carried out using sulfate precipitation from PACl (Shi et al., 2007; Xu et al., 2003). PACl solution (25 mL) and $NaSO_4$ (1.4204 g) were transferred into a colorimetric tube and diluted to 50 mL with deionised water. After 24 h of reaction, the samples were filtered and dried for 24 h. The filtrates were then collected and sealed in a glass bottle. To obtain a soluble Al_{13} product, 0.4 g of solid was placed in a 200 mL glass beaker, then 95.2 mL water and 4.8 mL 0.306 mol/L $Ba(NO_3)_2$ were added. Under intense agitation for 3 h, the insoluble product and soluble Al_{13} were separated by filtering through a 0.45 μm membrane. The filtrate Al concentration was measured using atomic absorption spectrometry.

2.2. Jar test procedure

Coagulation studies were performed in a conventional jar-test apparatus, equipped with six 1 L beakers. The stock HA solution was diluted with ionized water to reach the designated concentration of dissolved organic matter (DOC = 10 mg/L). Aluminum chloride ($AlCl_3 \cdot 6H_2O$) and purified Al_{13} were used in the study. The calculated volumes of coagulant (to achieve the required dosage) and 0.1 M tetramethylammonium hydroxide pentahydrate [$(CH_3)_4NOH \cdot 5H_2O$ (TMA)] solutions (to achieve the required pH) were added to the HA (DOC = 10 mg/L) solution. TMA was more useful than NaOH as base. This was because, while recording the ESI mass spectra, sodium formed several intense NaCl aggregate signals that interfered with the interpretation of the spectra (Sarpola et al., 2004). The coagulation procedure involved rapid mixing at 200 rpm for 1 min followed by slow stirring at 20 rpm for 30 min. After 50 s, approximately 10 mL solution was collected. The corresponding absorbance spectra were then recorded on a PERSEE TU-1901 UV/Vis spectrophotometer at wavelengths 200–600 nm. In addition, approximately 30 mL of the solution was taken to determine the Zeta potential by a laser Doppler electrophoresis apparatus (Malvern Zetasizer 90, UK). A 60 min settling period followed. Flocs were separated from the solution by centrifugation and lyophilised for solid ^{27}Al NMR analysis. The supernatant was filtered through a 0.22 μm membrane to test ESI-MS and measure DOC.

2.3. ESI-MS spectroscopy

To investigate aluminum hydrolysis at different pH values, fresh $AlCl_3$ and Al_{13} solutions were adjusted to different pH values by TMA or HCl solution, and immediately injected into the mass spectrometer.

ESI mass spectra were recorded with a Waters Xevo TQD mass spectrometer. All ESI-MS measurements were conducted in the positive ion mode. The sample solution was directly injected by a syringe pump at a flow rate of 5 μL/min into the ESI probe during flow injection analysis. The operating conditions were: capillary voltage, 3000 V; sample cone voltage, 70 V; extraction cone voltage, 5 V; source temperature, 110 °C; cone gas flow rate, 50 L/h; desolvation gas flow rate, 500 L/h.

2.4. Solid ^{27}Al NMR analysis

^{27}Al NMR spectra were obtained using a Bruker Advance 400 MHz NMR spectrometer equipped with a 5 mm resonance broadband observe probe. The main experimental parameters included 0.3 s of pulse width, recycle delays of 1 s, line broadening of 60 Hz, and spinning speed of 7 kHz.

2.5. DOC analysis

DOC was measured using a Shimadzu TOC-VC analyser. HCl was added to the samples, which were then sparged with CO_2-free air to strip inorganic carbon before catalytical platinum-aided combustion at 680 °C.

2.6. *Pyrolysis-gas chromatography-mass spectrometry*

Py-GC-MS was performed on freeze-dried flocs using a pyroprobe 5200 filament pyrolyser (CDS, Oxford) connected with a gas chromatograph mass spectrometer (QP2010 plus, Shimadzu). Freeze-dried floc samples were placed directly in the quartz tube. The quartz tubes underwent flash pyrolysis, and the platinum filament was programmed to a final temperature of 600 °C and held at this temperature for 20 s. The pyrolysis products were separated on an Rtx-5MS column (30 m × 0.25 mm, film thickness = 0.25 μm) using the following temperature conditions: 60 °C (1 min isothermal), raised to 300 °C at a rate of 10 °C/min, and held at 300 °C for 10 min. Helium was the carrier gas (1.0 mL/min), the injector temperature was 300 °C, and the split injection mode had an 80:1 split ratio. Pyrolysis products were detected by a mass spectrometer in the EI mode (70 eV) scanning from 30 to 500 amu.

2.7. *Other analytical measurements*

To statistically compare the data of the experiment, an analysis of variance (ANOVA) at the $p < 0.05$ significance level was conducted using IBM® SPSS® Statistics software (Version 20).

3. Results and discussion

3.1. *Removal characteristics of HA by $AlCl_3$ and preformed Al_{13}*

The removal efficiencies of HA by $AlCl_3$ and preformed Al_{13} as functions of pH and dosage are shown in Fig. 1.

The removal trends throughout the pH range investigated by $AlCl_3$ were similar. The removal efficiency of DOC increased significantly with increase in $AlCl_3$ dosage ($p < 0.05$, Table S1) and reached a steady state when the dosage was above the optimal dosage ($p > 0.05$, Table S1). However, pH significantly affected the coagulation efficiency. At optimal dosage of 6 mg/L, the removal increased first and then decreased as the pH increased. The maximum removal was reached at around pH 5–7, which was above 80%.

Preformed Al_{13} and $AlCl_3$ exhibited distinct coagulation behaviours in terms of DOC removal. As shown in Fig. 1, the removal efficiency of DOC of HA increased first and then decreased with dosage increased at pH 4–6 ($p < 0.05$, Table S2). At acidic conditons, the dosage at 4 mg/L contributed to the maximal DOC removal, which was approximately 72.3%, 78.9%, and 74.1% at pH 4, 5, and 6, respectively. Therefore, Al_{13} was less dependent on pH for removing DOC due to the presence of relatively stable aluminum species under acidic conditions. The coagulation performances at pH 7 and pH 8 were similar. DOC removal increased with Al dosage ($p < 0.05$, Table S2) and then approached a plateau ($p > 0.05$, Table S2), and the DOC removal was much efficient than that under acidic conditions when the aluminum dosage reached concentrations above 4 mg/L.

To investigate the compounds of HA removed by coagulation, the properties of the pyrolysis volatiles of HA flocs formed by $AlCl_3$ and Al_{13} coagulants at pH 5 and pH 7 were investigated. Fig. S1 shows the pyrolysis chromatogram for each of the samples, and their identified pyrolysis products are listed in Table S3-S6. The relative contents of the main compound groups are presented in Fig. 2. The compositions of pyrolysis volatiles are divided into ten main groups: polycyclic aromatic hydrocarbons (PAH), monocyclic aromatic hydrocarbons (MAH), aliphatic hydrocarbons (AH), nitrogenous heterocyclic compounds (NHP), hydrocarbon derivatives (HD), esters, amides, furans, nitriles, and others.

As shown in Fig. 2, aromatics (polycyclic aromatic hydrocarbons and monocyclic aromatic hydrocarbons) were the most abundant products that were the main structural components of HA. Compared to $AlCl_3$ coagulant, there were relatively higher contents of aromatics, esters, and amides, and lower contents of aliphatic hydrocarbons and hydrocarbon derivatives with Al_{13}. These results indicated that esters and amides were most efficiently removed by Al_{13}, while aliphatic hydrocarbons and hydrocarbon derivatives were most efficiently removed by $AlCl_3$. The significant quantitative differences were heterocyclic N-containing compounds, furans, and nitriles. Heterocyclic N-containing compounds were more abundant in $AlCl_3$ samples (5.5% at pH 5, 6% at pH 7) than in Al_{13} samples (1.5% at pH 5, 0% at pH 7). Furan was particularly scarce in Al_{13} sample (0.9% at pH 5) when compared to the $AlCl_3$ sample (6.6% at pH 5). Nitrile (accounted for 3.3%) was detected only in the Al_{13}

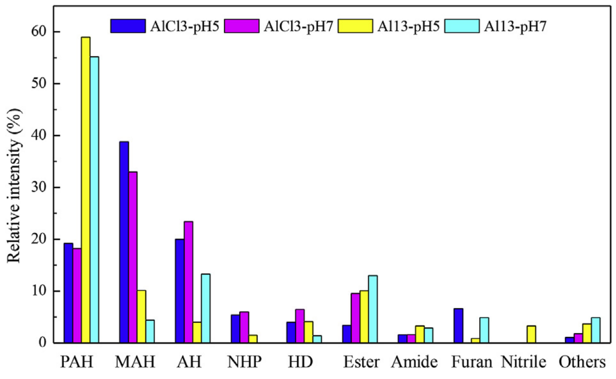

Fig. 2. Relative contents of the main groups of compounds identified by Py-GC–MS.

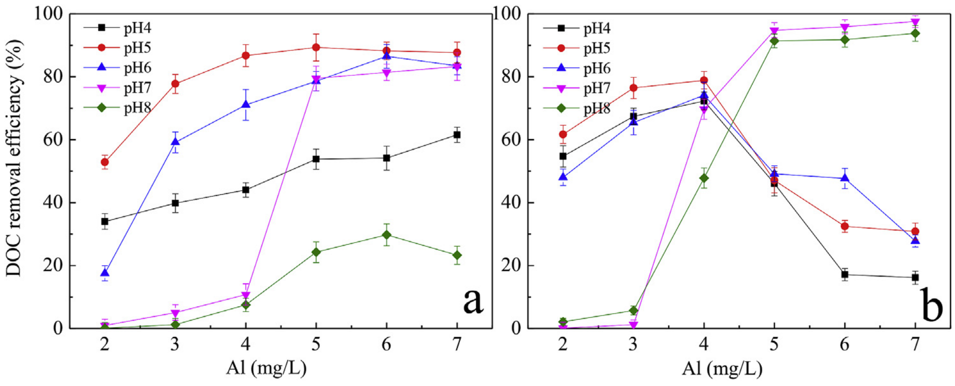

Fig. 1. Coagulation of HA with $AlCl_3$ (a) and Al_{13} (b) as functions of pH and dosage.

sample at pH 5, which indicated the selective removal of nitrile by Al_{13}. Heterocyclic N-containing compounds and furan were selectively removed from HA solution by $AlCl_3$ coagulant.

3.2. Characteristics of in situ aluminum hydrolysis and coagulation behaviours

pH has a great effect on the distribution of Al species. To investigate the effect of Al species on the coagulation process, ESI-MS spectra of $AlCl_3$ before and after coagulation with pH variation at dosage 6 mg/L are shown in Fig. 3. All the aluminum complexes identified in this study are generally described as $[Al_xO_y(OH)_z(H_2O)_m]^{(2y+z-3x)+}$.

Before coagulation, at pH 4.0, signals at m/z values 103 (20.44%), 121 (100%), 139 (80.2%), 157 (49.8%), and 175 (14.52%) dominated the ESI-MS spectra. These signals were assigned to the dimeric aluminum species $[Al_2O_2(OH)(H_2O)_{0\text{-}4}]^+$. Charged complexes with Al_1 cores (m/z 99, 115, and 133), Al_3 cores (m/z 163, 181, 199, 217, and 253), and Al_4 cores (m/z 81, 99, and 105) were also detected in the spectra. At pH 5.0, the aluminum salts further hydrolyzed and the aluminum speciation distribution changed significantly. The multi-charged Al_{13} complex series (m/z 328, 337, 355, 213, 219, 225) had the most intense signal series. A series of polymers containing Al_2, Al_4, Al_5, Al_9, and Al_{10} cores was also observed in the spectra at pH 5.0. When the pH was raised to 6.0, the signals of aluminum compounds decreased because of the formation of $Al(OH)_3$. The dimeric species (m/z 121, 139, 157, and 175) were the dominant species again in the spectrum. At pH 7.0, amorphous $Al(OH)_3$ was formed and the total ions decreased. The dimeric species (m/z 103, 121, and 139) were still the dominant species in the spectrum. According to the ESI-MS results discussed above, the aluminum species were classified into five categories as follows: monomeric and dimeric aluminum species (Al_1-Al_2), small polymeric aluminum species (Al_3-Al_5), median polymeric aluminum species (Al_6-Al_{10}), large polymeric aluminum species (Al_{11}-Al_{20}) and undetected part (i.e., $Al(OH)_3$ and/or $Al(OH)_4^-$) (Zhao et al., 2009a). The distribution of aluminum species before and after coagulation at different pH values are illustrated in Table 1.

As shown in Table 1, before coagulation, the monomeric and dimeric aluminum and small polymeric aluminum species decreased with the increase of pH, which was due to hydrolysis to form larger polymer or $Al(OH)_3$. Median polymer and large polymer increased firstly and reached maximum at pH 5, then decreased when the pH value was higher than 5. Undetected part mainly included $Al(OH)_3$ and $Al(OH)_4^-$. The content of undetected part increased and reached maximum of 90.56% at pH 7 due to formation of $Al(OH)_3$.

After coagulation (Fig. 3), the aluminum speciation distribution changed significantly at pH 4–6. The number of ion peaks with

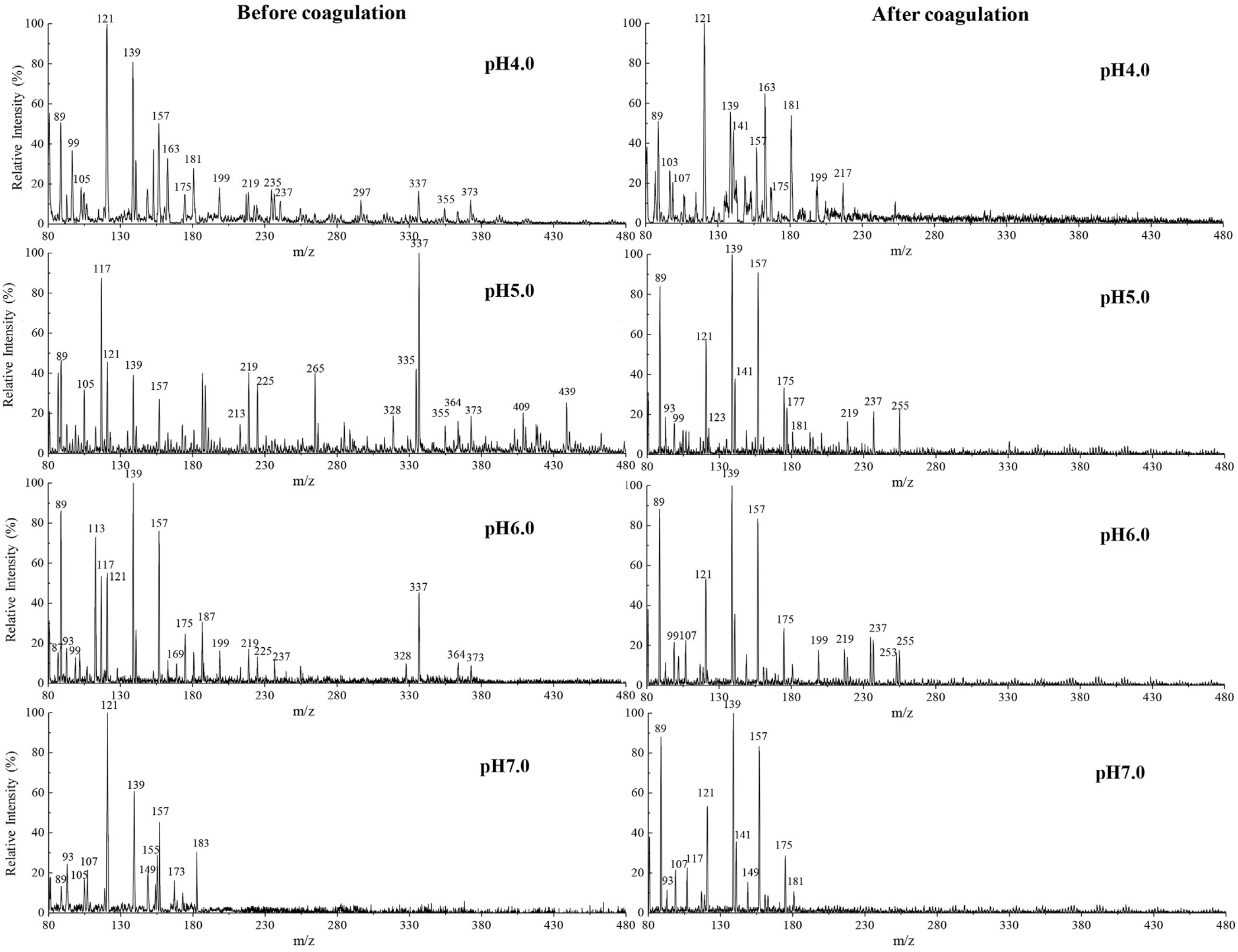

Fig. 3. ESI-MS spectra before and after coagulation at different pH values.

Table 1
Distribution of aluminum species before and after coagulation at different pH values for $AlCl_3$.

Aluminum species (%)	pH4		pH5		pH6		pH7	
	Before[a]	After[b]	Before	After	Before	After	Before	After
Monomer and dimer	46.94	43.56	10.09	35.67	17.56	25.46	4.85	5.34
Small polymer	34.8	45.12	22.25	47.46	19.74	29.65	2.8	4.98
Median polymer	12.22	10.16	24.4	10.31	12.25	5.34	1.79	1.23
Large polymer	6.04	1.16	43.26	6.56	10.3	2.13	0	0
Undetected part	0	0	0	0	40.15	37.42	90.56	88.45

[a] Before coagulation (Before).
[b] After coagulation (After).

higher m/z reduced remarkably, and relative intensity also decreased. For example, the polymeric aluminum species Al_{14}, Al_{15}, Al_{16}, and Al_{17} were diminished and Al_{13} species decreased significantly in the spectra at pH 5. Meanwhile, the relative content of large polymer decreased significantly (from 43.56% to 6.56%) (Table 1). Under acidic conditions, the removal of HA led to the complexation reaction between soluble cations and the functional groups of HA. This indicated that large polymeric species played an important role in the complexation reaction. Similar spectra were achieved before and after coagulation at pH 7. As shown in Table 1, the contents of different aluminium species before and after coagulation were quite similar. This can be attributed to the formation of $Al(OH)_{3(s)}$ as sweep coagulation occurred. This could be compared favourably to our previous investigations (Jin et al., 2018), which demonstrated that dosed Al remained unreacted until the dosage was increased to a critical value to form amorphous $Al(OH)_3$ at pH 7.

To further identify aluminum speciation during coagulation, HA flocs formed by $AlCl_3$ coagulant at pH 5 and pH 7 were collected and freeze-dried to obtain solid-state ^{27}Al NMR (Fig. 4).

The spectrum exhibited two distinctive resonances at about 2 ppm and 64 ppm at pH 5 (Fig. 4). The strong peak at 2 ppm corresponded to octahedrally coordinated aluminum. Many researchers have stated that this shift corresponds to 'free' Al dimers or complexed Al monomers and dimers (Zhao et al., 2009b). The 64 ppm signal was assigned to the tetrahedrally coordinated aluminum at the centre of Al_{13}, whose chemical shift was reported to be in the 61–64 ppm range, depending on the conditions of formation and aging (Liu et al., 2009). Signals from the other 12 shell-structured octahedral Al in Al were too broad to be detected by ^{27}Al NMR analysis. As a result, the concentration of Al_{13} in the NMR result needed to be multiplied by thirteen (Hiradate and Yamaguchi, 2003). Therefore, even though it seemed that the peak at 64 ppm had weak resonance, it was reasonable to confirm that the Al_{13} structure existed in the flocs formed by $AlCl_3$. Therefore, the possible Al species within the flocs were Al_{13} polymer, monomeric and dimeric aluminum. This suggested that the in situ formed Al_{13} and other hydrolyzed Al species could complex with HA and precipitate subsequently as flocs, namely in situ Al_{13} and other hydrolyzed Al species played synergistic effects in the removal of HA.

As shown in Fig. 4, the two spectra of $Al(OH)_{3(s)}$ and HA flocs formed at pH 7 (HA-$Al(OH)_3$) appeared similar. The peak at 2.4 ppm is assigned to AlO_6 octahedral coordination, 35 ppm to AlO_5 pentahedral coordination, and 65 ppm to AlO_4 tetragonal coordination (Isobe et al., 2003). Rämö et al. (2008) proposed that humic substances can be incorporated into $Al(OH)_{3(s)}$ crystal to form solid-state HS-Al complexes, which give rise to new ^{27}Al NMR signals. This study did not detect any new signals, indicating that soluble aluminum species hardly reacted with HA and adsorption of HA by $Al(OH)_{3(s)}$ was the main mechanism at pH 7. This observation is highly consistent with the results of ESI-MS and verifies the proposed coagulation mechanism at pH 7.

3.3. Hydrolzed species and coagulation behaviors of preformed Al_{13}

3.3.1. ESI-MS spectra of preformed Al_{13} at different pH values

Al_{13} species can be relatively stable after dosing in water as compared to $AlCl_3$ hydrolysis. The ESI-MS spectra of Al_{13} in the pH range 4.0–8.0 are shown in Fig. S2.

As shown in Fig. S2, the Al_{13} species at m/z 328, m/z 337, m/z 355, m/z 364, m/z 373, m/z 219, m/z 225, m/z 231, and m/z 237 dominated the spectra at pH 4.0–8.0. The total ion count (TIC) value was 1.0×10^7 under acidic conditions (pH 4.0–6.0). With pH value increased to 7.0 and 8.0, the total ions reduced, probably due to the formation of species undetected by ESI-MS (e.g., amorphous hydroxide solids). The TIC values for the same species decreased to 3.0×10^5 and 2.0×10^5. Although some of the aluminum species formed undetected species, Al_{13} was still the dominant species. This was similar to the results of Rämö et al. regarding the speciation of

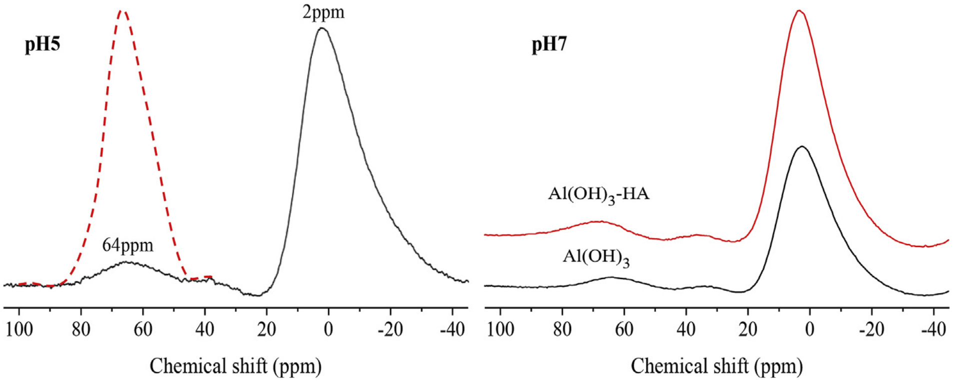

Fig. 4. ^{27}Al NMR spectra of freeze-dried flocs by $AlCl_3$ coagulation at pH 5 and pH 7.

highly basic polyaluminum (Rämö et al., 2008).

Polynuclear Al_{13} is a Keggin Al_{13}^{7+}-cation, $[AlO_4(Al(OH)_2)_{12}]^{7+}$ or $[Al_{13}O_4(OH)_{24}]^{7+}$, where the tetrahedral AlO_4 central unit is surrounded by twelve octahedral AlO_6 units in which the hydroxo groups are attached to the vertices of the octahedra. Al_{13} detected in the ESI-MS spectra is a species of forced hydrolysis formed by the addition of alkali. $AlCl_3$ could generate the Al_{13} polycation in situ by a spontaneous hydrolysis process. The following studies were carried out to investigate coagulation behaviors of preformed Al_{13} in order to compare the reactivity characteristics and mechanism of HA with in situ hydrolyzed and preformed Al species.

3.3.2. *Coagulation behaviors of preformed Al_{13}*

Based on ESI-MS results of preformed Al_{13}, the major detected aluminum species were the same Al_{13} species as those at pH 4.0–8.0. Thus, we chose pH 5 and pH 7 as typical pH values to compare the ESI-MS spectra before and after coagulation (Fig. 5).

As shown in Fig. 5, after coagulation, the aluminum speciation distribution was different from the initial Al_{13} species. The number of Al_{13} ion peaks reduced remarkably and the relative intensity also decreased. At pH 5, the peaks moved to a lower m/z range and Al_{13} also reduced. Al_2 (m/z 103, 121, 139, and 157), Al_7 (m/z 117, 123, 129, and 135), and Al_8 (m/z 137, 149, 155, and 167) species dominated the spectra. A series of small polymers containing Al_4, Al_5, Al_6, and Al_{10} species was also observed in the spectra after coagulation. There were similar changes at pH 7. It indicated that Al_{13} was not stable and decomposed into oligomeric and median polymeric species during coagulation. This could be compared favourably with the results of Hiradate and Yamaguchi, (2003), who observed that tetrahedral Al in Al-HA complexes gradually converted to octahedral Al, indicating that Al in Al-HA complexes decomposed to Al-HA complexes with reaction time.

3.4. *Complexation capacities of $AlCl_3$ and Al_{13} with HA*

HA is a major light-absorbing component in natural waters in the 200–800 nm range. The wide variety of light-absorbing functional groups (chromophores) in HA and the possible presence of complex intramolecular interactions result in absorbance spectra that are broad and featureless. Differential absorbance spectroscopy (DAS) is useful for detecting very subtle changes in NOM chemistry and has high sensitivity with low sample pretreatment (Dryer et al., 2008). In prior research, this technique has successfully been used to quantify NOM-metal interactions. Changes in the spectral slope in the range of wavelengths 325–375 nm ($DSlope_{325\text{-}375}$) in differential log-transformed absorbance spectra can be used to characterise the complexation between NOM and metal ions (Yan et al., 2013).

$DSlope_{325\text{-}375}$ parameters are given below (Zhou and Meng, 2016):

$$DSlope_{325-375} = Slope_{325-375,i} - Slope_{325-375,ref}$$

where $Slope_{325\text{-}375,i}$ is the slope of a straight line from 325 to 375 nm in the log-transformed absorbance at different aluminium concentrations, and $Slope_{325\text{-}375,ref}$ represents the parameter in the absence of aluminum.

Changes in the spectral parameters of $DSlope_{325\text{-}375}$ from HA by $AlCl_3$ and Al_{13} at different pH values as functions of the total concentration of added Al are shown in Fig. 6.

The $DSlope_{325\text{-}375}$ changes in HA because $AlCl_3$ and Al_{13} had distinctly different characteristics. For $AlCl_3$, it was observed that the $DSlope_{325\text{-}375}$ value positively correlated with the dosed aluminium in acidic conditions. Moreover, the curve increased rapidly ($p < 0.05$, Table S7) and then gradually reached steady states ($p > 0.05$, Table S7). At an Al concentration of 6 mg/L, the maximum $DSlope_{325\text{-}375}$ value was reached at pH 5, followed by pH 6 and pH 4. The corresponding $DSlope_{325\text{-}375}$ value were 0.0019, 0.0024 and 0.0021 at pH 4, 5 and 6, respectively. At $pH \geq 7$, the $DSlope_{325\text{-}375}$ value was obviously lower than 0.0006 and there was no significant variation with increase in dosage ($p > 0.05$, Table S7). For Al_{13}, the whole change trends of $DSlope_{325\text{-}375}$ were similar in the range of pH 4–8. The value of $DSlope_{325\text{-}375}$ increased and subsequently decreased when the Al_{13} dosage increased ($p < 0.05$, Table S8). While the dosage required to reach the maximum $DSlope_{325\text{-}375}$ at $pH \geq 7$ was higher than that in acidic conditions.

$DSlope_{325\text{-}375}$ was independent of HA concentration and provided the extent of metal-DOM binding (Yan et al., 2013). Based on the above results, the complexation reaction characteristics of $AlCl_3$ and Al_{13} with HA were significantly different. For $AlCl_3$, higher value of $DSlope_{325\text{-}375}$ indicated that high reactivity between HA and Al occurred at $pH < 7$. The best degree of complexation was reached at pH 5.0. By contrast, the added aluminum hardly reacted with HA at $pH \geq 7$. However, complexation occurred between HA and Al_{13} coagulant at all pH values tested.

3.5. *Mechanisms of HA removal by $AlCl_3$ and Al_{13}*

3.5.1. *Continuous multiligand distribution model to evaluate metal binding sites in humic materials*

Continuous multiligand distribution model have been reported elsewhere (Dobbs et al., 1989; Grimm et al., 1991) and shown in supporting information. The normal distribution curves of binding site at different pH values are shown in Fig. 7.

The abscissa and ordinate in Fig. 7 refer to the conditional stability constant and L_B/L_T, respectively. Aluminum binding site distributions in humic materials were distinct at different pH levels. The higher the proton concentration, the weaker the effective complex formation strengths, and the narrower the effective width of the distribution of the binding sites. Under acidic conditions, the binding site distribution gradually agreed with the normal distribution, and the effective width of binding site distribution increased progressively with pH increased. This indicated that the binding sites occupied by metal ions increased as the pH increased from 3 to 6. The area under the upper curve in the graph represented the amount of binding sites. At low pH, a significant portion of binding sites was occupied by protons. Al^{3+} ions competed with protons to form complexes. The proton migration of functional groups reduced due to the large proton concentration in solution. Therefore, most of the binding sites were occupied by protons. As the pH increased, Al^{3+} was more strongly bound to the binding sites as the deprotonation of functional groups increased. Most of the binding sites are occupied by the metal ion. Therefore, the amount of bound aluminum reached maximum at pH 5–6. At $pH \geq 7$, the distribution of the binding sites appeared broader and the binding sites occupied by metal ions decreased.

In addition, the conditional stability constants at pH 5.0 was much larger than that at pH 7.0, which proved that aluminum ions tended to combine with the functional groups on the HA molecules and form Al-HA complexes at pH 5.0.

3.5.2. *Analysis of mechanisms*

The reactivity characteristics and mechanism of humic acid with $AlCl_3$ and performed Al_{13} can be interpreted as shown in Fig. 8.

As is well known, the removal of HA was due to complexation between aluminum ions and HA under acidic conditions (Jin et al., 2018). $AlCl_3$ can be hydrolyzed to various Al species in aqueous solution depending on the pH. The distributions of binding site in HA could be change due to protonation/deprotonation of functional groups of HA. Therefore, the coagulation efficiency was attributed to differences in Al species and the amount of aluminum bound to

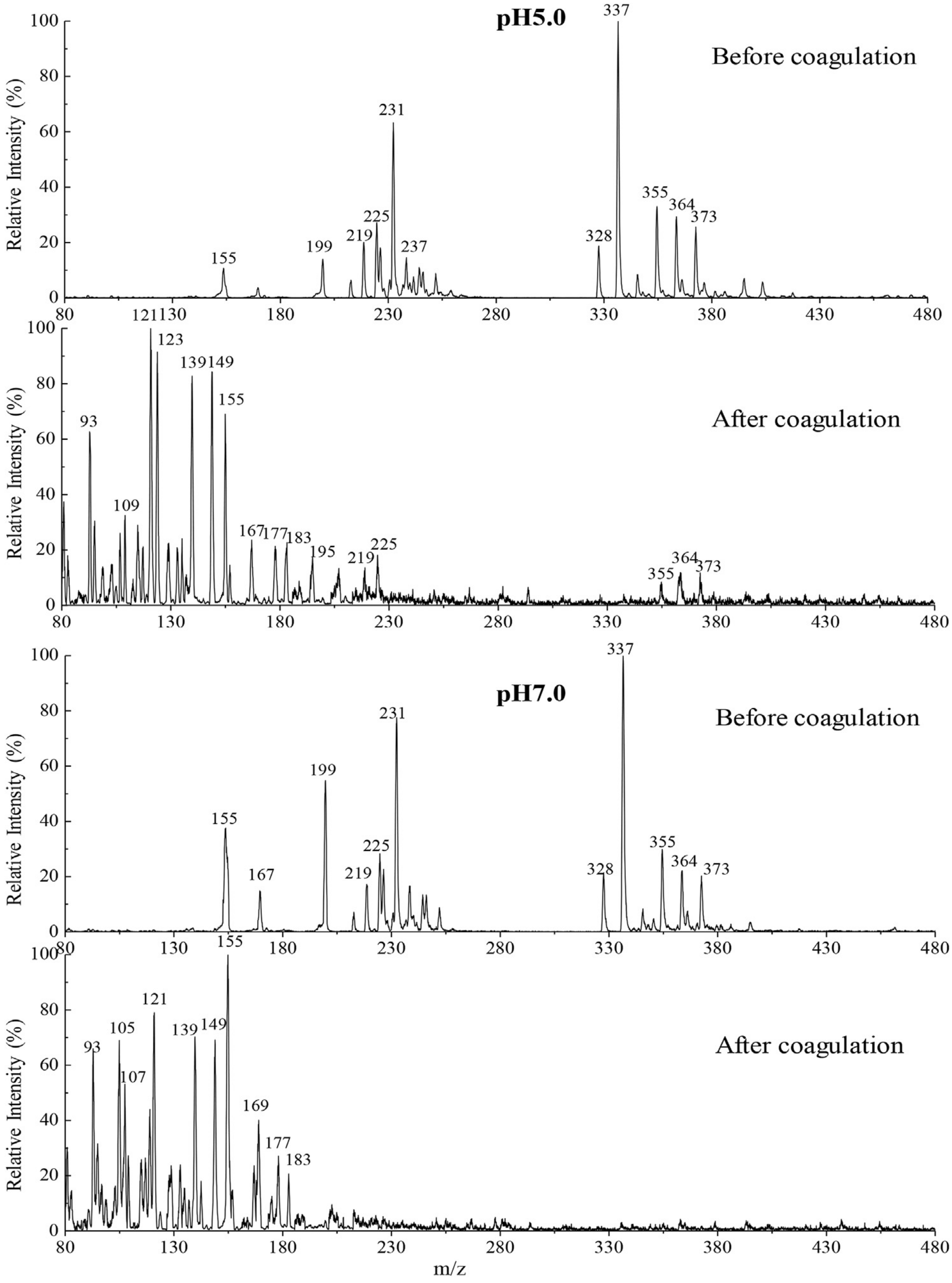

Fig. 5. ESI-MS spectra before and after coagulation by Al_{13} at pH 5 and pH 7.

HA. For $AlCl_3$, the dominating Al species at pH 4 were dimer, monomer, and other oligomers, which had a certain complexation ability and HA removal. Although the charge of the dimer was not as high as that of Al_{13}, the charge per Al ion in the dimer was higher than that in Al_{13} (Yan et al., 2008b). The maximum level of HA removal was reached at pH 5 to 6, which was higher than that for preformed Al_{13}. At pH 5–6, $AlCl_3$ hydrolyzed to form various aluminum species, including dimer, small polymer, larger polymer (i.e., in situ Al_{13}) and so on. Due to the diversity of the hydrolyzed Al species and discrepancy in the binding site distributions of HA, the binding sites of HA with different affinities selectively bound with diverse Al species, which increased the complexing probability of the binding sites of HA. Yan et al. (2007) concluded that the removal of unsatisfied coordinate bonds of organic matter correlated with the content of Al_b (mainly Al_{13}) while the removal of aromatic compounds (UV_{254}) was determined by the content of Alc (mainly $Al(OH)_3$). Zhao et al. (2009b) concluded that monomer aluminum was preferentially bound to polysaccharides and cellulosic molecules, whereas preformed Al_{13} species selectively bound to carboxylic groups at pH 6.0. In addition, complexation capacity of $AlCl_3$ was higher than that of Al_{13} at the optimum dosage. The values of $DSlope_{325-375}$ for $AlCl_3$ and Al_{13} were determined to be 0.0024 and 0.0020, respectively. Therefore, the synergistic effects of various in situ hydrolyzed Al species with higher complexation capacity played important roles in removing HA at pH 5–6.

According to Py-GC-MS analysis, compared to the $AlCl_3$ sample, the products of the Al_{13} sample had a higher content of aromatics at pH 5. As a result, relatively lower proportions of other compounds in HA could be removed by the Al_{13} coagulant. Moreover, performed Al_{13} could gradually be converted to octahedral Al during

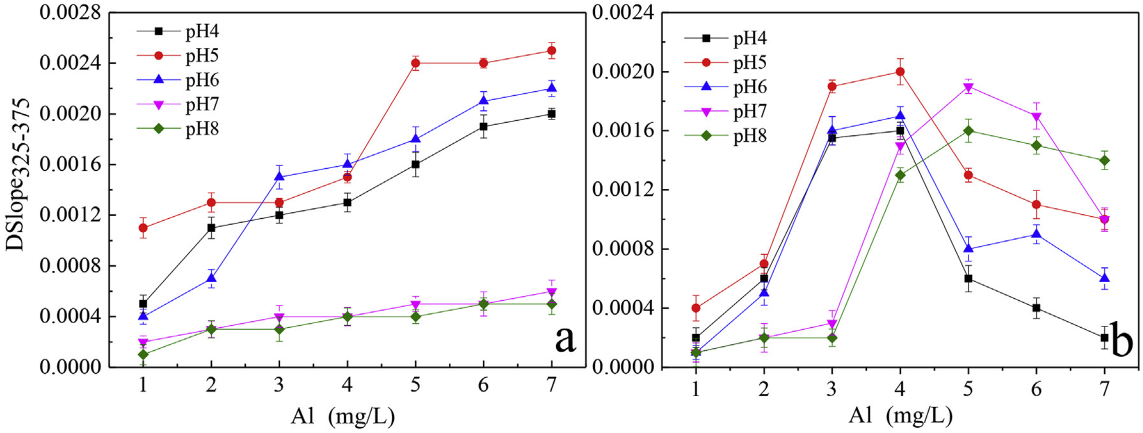

Fig. 6. Changes in spectral parameters of $DSlope_{325-375}$ from HA at different pH values as functions of the total concentration of added Al (a) $AlCl_3$; (b) Al_{13}.

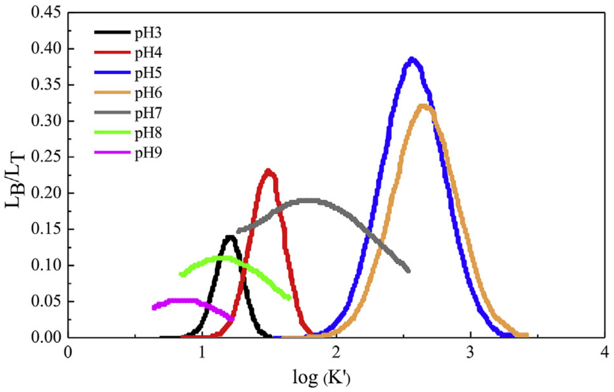

Fig. 7. Continuous multiligand distribution model at different pH levels.

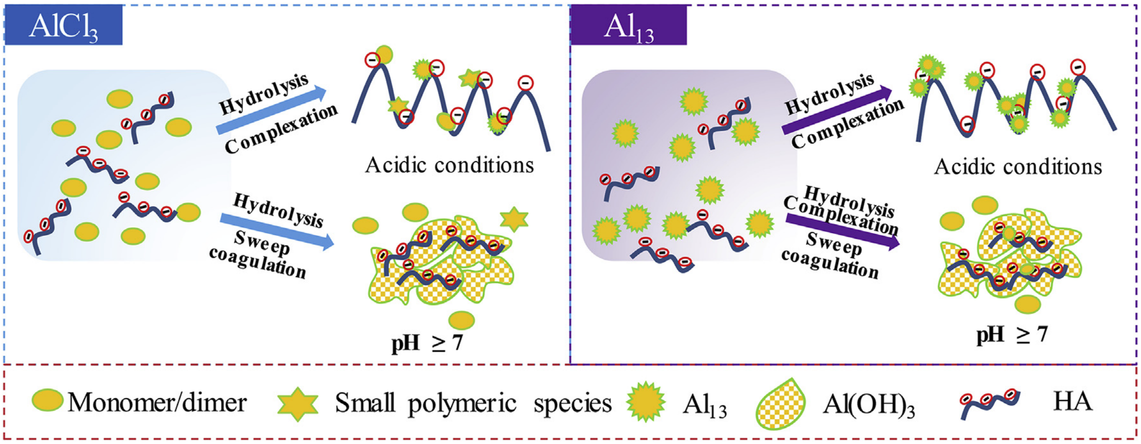

Fig. 8. Reactivity characteristics and mechanism of humic acid with $AlCl_3$ and Al_{13}.

coagulation and had less complexation capacity with HA, affecting coagulation efficiency. Fig. S3 shows the Zeta potential at different Al_{13} dosage at pH 5. For preformed Al_{13}, the Zeta potential increased sharply at lower dosage and shifted to the positive region with increase in Al_{13} dosage. Therefore, preformed Al_{13} with high positive charges could not completely neutralise the negative binding sites of HA with lower charge density. This resulted in charge reversal and the formation of electrostatic patches. The higher degree of binding consumed or covered some of the binding sites, which made it difficult for flocs to aggregate. Al_b could thus destabilise the particles efficiently to form aggregates. However, it could not form flocs that were large enough to settle efficiently, and remained mostly in colloidal form (Yan et al., 2007).

The coagulation mechanisms of HA by $AlCl_3$ were distinctly different from those of Al_{13} at pH ≥ 7. For $AlCl_3$, $Al(OH)_3$ were the major species and some oligomers were also formed. However, most oligomers did not react with HA and almost all HA was removed via sweep flocculation. Therefore, the dominant coagulation mechanism was the adsorption of HA on amorphous $Al(OH)_3$ for $AlCl_3$. The value of $DSlope_{325-375}$ for preformed Al_{13} indicated that complexation occurred between HA and preformed Al_{13}. Therefore, complexation and sweep coagulation were involved in the coagulation of HA by Al_{13}. These resulted in higher HA removal efficiency obtained at pH ≥ 7 in Al_{13} coagulation.

4. Conclusions

In this study, the synergistic effects of various in situ hydrolyzed aluminum hydrolysis and coagulation behavior of in situ and preformed Al species for the removal humic acid (HA) were investigated. For $AlCl_3$, the DOC removal was strongly related to the pH values. The maximum HA removal reached at weak acidic conditions, where various in situ hydrolyzed Al species containing Al_1 to Al_{20} cores with different amounts of water molecules were present.

Meanwhile, the binding site distributions of HA were distinct with variations in pH, which brought about different affinities with the Al species. Because of the diversity of in situ hydrolyzed aluminium species and discrepancy in the binding sites of HA, various Al species could meet the demand for different binding sites and enhance the complexing probability. Therefore, the synergistic effects of various in situ hydrolyzed aluminium species played important roles in the removal of HA. Compared with $AlCl_3$, Al_{13} was less dependent on pH to remove HA due to the simplex preformed Al species. Under weak acidic conditions, the Zeta potential of HA formed by preformed Al_{13} increased from negative to positive with increase in Al_{13} dosage, resulting in charge reversal and partial supersaturation of sites. As a result, HA was removed inefficiently. Moreover, Al_{13} could gradually be converted to octahedral Al during coagulation and had less complexation capacity with HA, affecting coagulation efficiency.

Acknowledgements

This study was financially supported by the National Key Technology Support Program (Grant No. 2014BAC13B06), the National Natural Science Foundation of China (Grant No. 51378414, 51178376), the Program for Innovative Research Team in Shaanxi (Grant No. 2013KCT-13) and the Program for New Century Excellent Talents in the University of Ministry of Education of China (NCET-12-1043).

Appendix A. Supplementary data

Supplementary data to this article can be found online at https://doi.org/10.1016/j.watres.2018.10.039.

References

Angelico, R., Cegliea, A., He, J.Z., Liu, Y.R., Palumboa, G., Colombo, C., 2014. Particle size, charge and colloidal stability of humic acids coprecipitated with ferrihydrite. Chemosphere 99, 239–247.

Bahemmat, M., Farahbakhsh, M., Kianirad, M., 2016. Humic substances-enhanced electroremediation of heavy metals contaminated soil. J. Hazard Mater. 312, 307–318.

Benschoten, J.E.V., Edzwald, J.K., 1990. Chemical aspects of coagulation using aluminum salts-II. Coagulation of fulvic-acid using alum and polyaluminum chloride. Water Res. 24, 1527–1535.

Black, A.P., Chen, C.L., 1965. Electrophoretic studies of coagulation and flocculation of river sediment suspensions with aluminum sulfate. J. AWWA 57 (3), 354–362.

Cheng, W.P., Chi, F.H., 2002. A study of coagulation mechanisms of polyferric sulfatereacting with humic acid using a fluorescence-quenching method. Water Res. 36, 4583–4591.

Dobbs, J.C., Susetyo, W., Carreira, L.A., Azarraga, L.V., 1989. Competitive binding of protons and metal ions in humic substances by lanthanide ion probe spectroscopy. Anal. Chem. 61, 1519–1524.

Dryer, D.J., Korshin, G.V., Fabbricino, M., 2008. In situ examination of the protonation behavior of fulvic acids using differential absorbance spectroscopy. Environ. Sci. Technol. 42, 6644–6649.

Grimm, D.M., Azarraga, L.V., Carreira, L.A., Susetyo, W., 1991. Continuous multiligand distribution model used to predict the stability constant of Cu(II) metal complexation with humic material from fluorescence quenching data. Environ. Sci. Technol. 25 (8), 1427–1431.

Hiradate, S., Yamaguchi, N.U., 2003. Chemical species of Al reacting with soil humic acids. J. Inorg. Biochem. **9**7, 26–31.

Isobe, T., Watanabe, T., d'Espinose, J.B., Legrand, A.P., Massiot, D., 2003. Solid-state ^1H and ^{27}Al NMR studies of amorphous aluminum hydroxides. J. Colloid Interface Sci. 261, 320–324.

Jin, P.K., Song, J.N., Yang, L., Jin, X., Wang, X.C., 2018. Selective binding behavior of humic acid removal by aluminum coagulation. Environ. Pollut. 233, 290–298.

Lin, J.-L., Huang, C., Dempsey, B.A., Hu, J.-Y., 2014. Fate of hydrolyzed Al species in humic acid coagulation. Water Res. 56, 314–324.

Liu, H.J., Hu, C.Z., Zhao, H., Qu, J.H., 2009. Coagulation of humic acid by PACl with high content of Al_{13}: the role of aluminum speciation. Separ. Purif. Technol. 70, 225–230.

Lu, X.Q., Chen, Z.L., Yang, X.H., 1999. Spcetrosopic study of aluminium speciation in removing humic substances by Al coagulation. Water Res. 33 (5), 3271–3280.

Packham, R.F., 1963. Studies of organic colour in natural water. Proc. Soc. Water Treat. Exam. 12, 15.

Rämö, J.H., Sarpola, A.T., Hellman, A.H., Leiviskä, T.A., Hietapelto, V.K., Jokela, J.T., Laitinen, R.S., 2008. Colloidal surfaces and oligomeric species generated by water treatment chemicals. Chem. Speciat. Bioavailab. 20 (1), 13–22.

Randtke, S.J., 1988. Organic comtaminant removal by coagulation and related process combinations. J. AWWA 80 (5), 40–56.

Sarpola, A., Hietapelto, V., Jalonen, J., Jokela, J., Laitinen, R.S., 2004. Identification of the hydrolysis products of $AlCl_3 \cdot 6H_2O$ by electrospray ionization mass spectrometry. J. Mass Spectrom. 39, 423–430.

Shi, B.Y., Li, G.H., Wang, D.S., Tang, H.X., 2007. Separation of Al_{13} from polyaluminum chloride by sulfate precipitation and nitrate metathesis. Separ. Purif. Technol. 54, 88–95.

Singley, J.E., Yao, K.M., Miller, D.G., Gordam, G.R., Cleasby, J.L., 1971. State of the art of coagulation. J. AWWA 63 (2), 99–108.

Tang, H.X., Luan, Z.K., 1995. Features and mechanism for coagulation flocculation processes of polyaluminum chloride. J. Environ. Sci. 7, 204–211.

Xu, Y., Wang, D.S., Liu, H., Lu, Y.Q., Tang, H.X., 2003. Optimization of the separation and purification of Al_{13}. Colloids Surf., A 231, 1–9.

Xu, W.N., Gao, B.Y., Yue, Q.Y., Wang, Y., 2010. Effect of shear force and solution pH on flocs breakage and re-growth formed by nano-Al_{13} polymer. Water Res. 44, 1893–1899.

Xu, W.Y., Gao, B.Y., Yue, Q.Y., Wang, Q., 2011. Effect of preformed and non-preformed Al_{13} species on evolution of floc size, strength and fractal nature of humic acid flocs in coagulation process. Separ. Purif. Technol. 78, 83–90.

Yan, M.Y., Wang, D.S., Qu, J.H., He, W.J., Chow, C.W., 2007. Relative importance of hydrolyzed Al(III) species (Al_a, Al_b, and Al_c) during coagulation with polyaluminum chloride: a case study with the typical micro-polluted source waters. J. Colloid Interface Sci. 316, 482–489.

Yan, M.Q., Wang, D.S., Qu, J.H., Ni, J.R., Chow, C.W.K., 2008a. Enhanced coagulation for high alkalinity and micro-polluted water: the third way through coagulant optimization. Water Res. 42, 2278–2286.

Yan, M.Q., Wang, D.S., Ni, J.R., Qu, J.H., Chow, C.W.K., Liu, H.L., 2008b. Mechanism of natural organic matter removal by polyaluminum chloride: effect of coagulant particle size and hydrolysis kinetics. Water Res. 42, 3361–3370.

Yan, M.Q., Wang, D.S., Korshin, G.V., Benedetti, M.F., 2013. Quantifying metal ions binding onto dissolved organic matter using log-transformed absorbance spectra. Water Res. 47, 2603–2611.

Zhao, H., Liu, H.J., Hu, C.Z., Qu, J.H., 2009a. Effect of pH on the aluminum salts hydrolysis during coagulation process: formation and decomposition of polymeric aluminum species. J. Colloid Interface Sci. 330, 105–112.

Zhao, H., Liu, H.J., Hu, C.Z., Qu, J.H., 2009b. Effect of aluminum speciation and structure characterization on preferential removal of disinfection byproduct precursors by aluminum hydroxide coagulation. Environ. Sci. Technol. 43, 5067–5072.

Zhou, M.G., Meng, F.G., 2016. Aluminum-induced changes in properties and fouling propensity of DOM solutions revealed by UV-vis absorbance spectral parameters. Water Res. 93, 153–162.